JACS
JOURNAL OF THE AMERICAN CHEMICAL SOCIETY
Article
pubs.acs.org/JACS

Selenium as a Structural Surrogate of Sulfur: Template-Assisted Assembly of Five Types of Tungsten–Iron–Sulfur/Selenium Clusters and the Structural Fate of Chalcogenide Reactants

Bo Zheng, Xu-Dong Chen, Shao-Liang Zheng, and R. H. Holm*

Department of Chemistry and Chemical Biology, Harvard University, Cambridge, Massachusetts 02138, United States

Supporting Information

ABSTRACT: Syntheses of five types of tungsten–iron–sulfur/selenium clusters, namely, incomplete cubanes, single cubanes, edge-bridged double cubanes (EBDCs), P^N-type clusters, and double-cuboidal clusters, have been devised using the concept of template-assisted assembly. The template reactant is six-coordinate $[(Tp^*)W^{VI}S_3]^{1-}$ [Tp* = tris(3,5-dimethylpyrazolyl)-hydroborate(1−)], which in the assembly systems organizes $Fe^{2+/3+}$ and sulfide/selenide into cuboidal $[(Tp^*)WFe_2S_3]$ or cubane $[(Tp^*)WFe_3S_3Q]$ (Q = S, Se) units. With appropriate terminal iron ligation, these units are capable of independent existence or may be transformed into higher-nuclearity species. Selenide is used as a surrogate for sulfide in cluster assembly in order to determine by X-ray structures the position occupied by an external chalcogenide nucleophile or an internal chalcogenide atom in the product clusters. Specific incorporation of selenide is demonstrated by the formation of $[WFe_3S_3Se]^{2+/3+}$ cubane cores. Reductive dimerization of the cubane leads to the EBDC core $[W_2Fe_6S_6Se_2]^{2+}$ containing μ_4-Se sites. Reaction of these species with HSe^- affords the P^N-type cores $[W_2Fe_6S_6Se_3]^{1+}$, in which selenide occupies μ_6-Se and μ_2-Se sites. The reaction of $[(Tp^*)WS_3]^{1-}$, $FeCl_2$, and Na_2Se yields the double-cuboidal $[W_2Fe_4S_6Se_3]^{2+/0}$ core with μ_2-Se and μ_4-Se bridges. It is highly probable that in analogous sulfide-only assembly systems, external and internal sulfide reactants occupy corresponding positions in the cluster products. The results further demonstrate the viability of template-assisted cluster synthesis inasmuch as the reduced $(Tp^*)WS_3$ unit is present in all of the clusters. Structures, zero-field Mössbauer data, and redox potentials are presented for each cluster type.

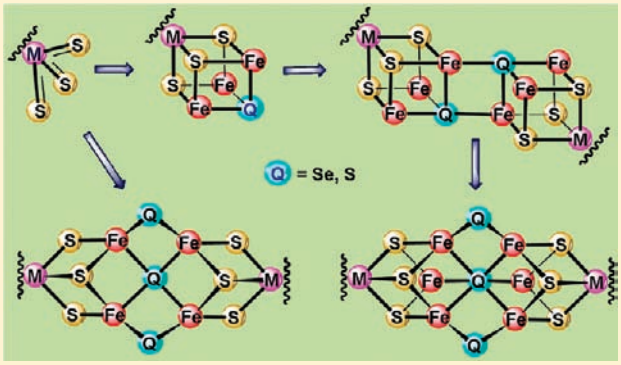

INTRODUCTION

Metal cluster self-assembly proceeds by self-organizing reactions between mononuclear precursors and ligand reactants in the initial step.[1] We recently demonstrated a new method of cluster assembly leading to weak-field heterometal cubane-type core units $[MFe_3S_3Q]^{2+/3+}$ (M = Mo, W; Q = S, Se). In comparison with earlier assembly procedures,[1−3] this method has two distinguishing features: (i) The system contains a template reactant of the general type $[L_3M^{VI}S_3]^{0/1-}$, in which L_3 is a facial tridentate ligand that blocks three coordination sites and provides a discrete coordination unit. Reduction to the $M^{III,IV}$ level in the assembly reaction system facilitates the binding of three $Fe^{II,III}$ atoms in the formation of the cluster product. (ii) Because the template reactant supplies three sulfur atoms, a fourth chalcogenide atom as a separate reactant can be specifically incorporated in cubane clusters as μ_3-Q. The first template ligand employed for this purpose was the cyclic triamine Bu^t_3tach,[4] which supports the formation of the cubane clusters $[(Bu^t_3tach)MFe_3S_3QL_3]^{0/1-}$ (L = Cl^-, RS^-).[5]

Single cubanes are precursors to higher-nuclearity clusters that are participants in attempts to achieve synthetic representations of large biological clusters such as the P^N and FeMo-cofactor clusters of nitrogenase[6−10] and the C-cluster of nickel-containing carbon monoxide dehydrogenase.[11−13] Clusters elaborated from single cubanes are primarily edge-bridged double cubanes (EBDCs) $[M_2Fe_6(\mu_3\text{-}S)_6(\mu_4\text{-}S)_2]$ and P^N-type clusters $[M_2Fe_6(\mu_2\text{-}S)_2(\mu_3\text{-}S)_6(\mu_6\text{-}S)]$ (M = Mo,[14−18] V[19,20]) with the indicated bridge connectivities (see below).

To examine the scope of template-based assembly, we utilized $[(Tp^*)WS_3]^{1-}$ [Tp* = tris(3,5-dimethylpyrazolyl)-hydroborate(1−)], which is readily obtained from $[(Tp^*)W(CO)_3]^{1-}$ and elemental sulfur.[21a] Earlier we showed that this reactant assembles certain $[WFe_3S_4]$ clusters.[22] The complex has also been shown to form dinuclear complexes with other metal species.[21] This report provides a much more extensive examination of this reactivity, including conversion of single cubanes into higher-nuclearity clusters, among which is a new type not previously obtained in this way. Additionally, as a surrogate marker for sulfide, we utilized selenide as an added reactant in the cluster synthesis or present in the core of a precursor cluster. The fate of selenide in the product cluster implies a corresponding role for sulfide. As will be seen, this approach supports the template interpretation of single-cubane

Received: February 10, 2012
Published: March 16, 2012

   dx.doi.org/10.1021/ja3010539 | J. Am. Chem. Soc. 2012, 134, 6479–6490

assembly systems and provides additional insight into cluster formation.

EXPERIMENTAL SECTION

Preparation of Compounds. All reactions and manipulations were performed under a dinitrogen atmosphere. Volume reduction and drying steps were carried out in vacuo; filtrations were through Celite. Commercial-grade chemicals were used without further purification. Unless otherwise indicated, $FeCl_2$, NaSEt, and Na_2Se were used as suspensions in the indicated solvents. Tetrahydrofuran (THF) and diethyl ether were purified using an Innovative Technology or MBraun solvent purification system. *N*,*N*-Dimethylformamide (DMF) was dried over molecular sieves for 24 h. Compounds were identified by combinations of elemental analysis (Midwest Microlab, LLC, Indianapolis, IN), ^{1}H NMR spectra, and in nearly all cases X-ray structure determinations. Chemical shifts of counterions are not included in the ^{1}H NMR data below. In some cases, some of the proton signals were not located because of paramagnetic broadening or overlap with cation or solvent signals; certain very broad (vbr) signals that were not easily assigned are noted. Analytical results indicated that some compounds crystallized as solvates; solvate components were detected in the ^{1}H NMR spectra. Because of the tendency of some compounds to desolvate, yields were calculated for the unsolvated compounds.

The compounds $(Et_4N)[(Tp^*)WFe_3S_4Cl_3]$ (δ −1.53 (3), 4.65 (1), 17.7 (br, 3)) and $(Et_4N)[(Tp^*)WFe_3S_4(SEt)_3]$ (δ −0.53 (9), 4.91 (3), 5.36 (9), 16.7 (br, 9), 47.4 (br, 6) were prepared as described elsewhere.[22]

A. Incomplete Cubanes. *$(Et_4N)[(Tp^*)WFeS_3Cl_2]$.* To a solution of 1.00 g (1.41 mmol) of $(Et_4N)[(Tp^*)WS_3]$[21] in 65 mL of acetonitrile was added a slurry of 179 mg (1.41 mmol) of $FeCl_2$ in 5 mL of acetonitrile. The dark-red reaction mixture was stirred for 48 h and filtered. The filtrate was reduced to dryness, and the residue was recrystallized from acetonitrile/ether to give the product as 990 mg (84%) of dark-red crystals. ^{1}H NMR (CD_3CN): δ 0.29 (br, 3), 3.79 (br, 3). Anal. Calcd for $C_{23}H_{42}BCl_2FeN_7S_3W{\cdot}CH_3CN$: C, 34.31; H, 5.18; N, 12.80. Found: C, 34.43; H, 5.00; N, 12.72.

$(Et_4N)[(Tp^*)WFe_2S_3Cl_2(SEt)]$. To a solution of 80 mg (0.11 mmol) of $(Et_4N)[(Tp^*)WS_3]$ in 3 mL of acetonitrile was added a solution of 28 mg (0.23 mmol) of $FeCl_2$ in 0.5 mL of methanol. After 1 min, a solution of 19 mg (0.23 mmol) of NaSEt in 0.5 mL of methanol was added. The mixture was stirred for 2 h and filtered. Slow diffusion of ether into the filtrate resulted in the formation of a solid, which was washed with ether to yield the product as 67 mg (64%) of black platelike crystals. ^{1}H NMR: δ −30.5 (br, ∼3), −11.57 (3), −7.76 (6), −1.93 (2), 0.10 (1), 1.17 (2), 5.09 (1). Additional signals were observed at δ 62 (vbr) and 106 (vbr). Anal. Calcd for $C_{25}H_{47}BCl_2Fe_2N_7S_4W$: C, 31.57; H, 4.98; N, 10.31. Found: C, 31.74; H, 5.03; 10.07. This procedure affords a purer product than that reported earlier.[22]

$(Et_4N)[(Tp^*)WFe_2S_3(SEt)_3]$. To a solution of 100 mg (0.10 mmol) of $(Et_4N)[WFe_2S_3Cl_2(SEt)]$ in 4 mL of acetonitrile was added 18 mg (0.21 mmol) of NaSEt in 2 mL of acetonitrile. The mixture was stirred for 2 h and filtered, and ether was diffused into the filtrate. The product was obtained as 49 mg (49%) of black crystals. ^{1}H NMR (CD_3CN, anion): δ −32.1 (br, 3), −8.75 (3), −7.18 (6), −2.95 (2), 0.27 (1), 3.49 (1), 5.17 (br, 2), 29.0 (br, ∼6). Additional signals were observed at δ 58 and 100.

B. Single Cubanes. *$(Et_4N)[(Tp^*)WFe_3S_3SeCl_3]$.* **Method 1.** To a solution of 900 mg (1.27 mmol) of $(Et_4N)[(Tp^*)WS_3]$ in 150 mL of acetonitrile was added a slurry of 518 mg (4.07 mmol) of $FeCl_2$ in 30 mL of THF. After 3 min, a suspension of 322 mg (2.54 mmol) of Na_2Se in 30 mL of THF was introduced. The black reaction mixture was stirred for 30 h and filtered. The filtrate was reduced to dryness. The residue was recrystallized from acetonitrile/ether to give the product as 875 mg (64%) of black needlelike crystals. ^{1}H NMR (CD_3CN, anion): δ −1.53 (3), 4.58 (1), 17.4 (br, 3). Anal. Calcd for $C_{23}H_{42}BCl_3Fe_3N_7S_3SeW$: C, 26.05; H, 3.99; N, 9.25. Found: C, 26.37; H, 4.06; N, 9.16.

Method 2. To a solution of 100 mg (0.12 mmol) of $(Et_4N)[(Tp^*)WFeS_3Cl_2]$ in 40 mL of acetonitrile was added 49 mg (0.38 mmol) of $FeCl_2$ in 20 mL of THF. After 2 min, 32 mg (0.24 mmol) of Na_2Se in 20 mL of THF was introduced. The black reaction mixture was stirred for 36 h and filtered, and the dark filtrate was reduced to dryness. The black residue was recrystallized from acetonitrile/ether to give the product as 97 mg (77%) of black needlelike crystals whose ^{1}H NMR spectrum was identical to the product obtained using method 1.

$(Et_4N)[(Tp^*)WFe_3S_3Se(SEt)_3]$. To a solution of 64 mg (0.06 mmol) of $(Et_4N)[(Tp^*)WFe_3S_3SeCl_3]$ in 1 mL of acetonitrile was added 18 mg (0.21 mmol) of NaSEt in 2.5 mL of acetonitrile. The reaction mixture was stirred for 2 h and filtered. Diffusion of ether into the filtrate caused the separation of a solid, which was washed with ether to afford the product as 42 mg (61%) of black crystals. ^{1}H NMR (CD_3CN, anion): δ −0.64 (9), 2.77 (3), 4.81 (3), 5.47 (6), 15.34 (2), 16.7 (br, 9), 48.5 (br, 4).

$[(Tp^*)WFe_3S_4(PEt_3)_3](BPh_4)$. To a solution of 608 mg (0.60 mmol) of $(Et_4N)[(Tp^*)WFe_3S_4Cl_3]$ in 40 mL of acetonitrile was added 352 mg (2.98 mmol) of PEt_3. After 1 min, a solution of 1.19 g (3.48 mmol) of $NaBPh_4$ in 6 mL of acetonitrile was introduced. The black solution was stirred for 24 h, and 130 mL of ether was added. The mixture was stirred for 5 h and filtered, and the filtrate was reduced to dryness. The residue was extracted with dichloromethane and benzene. Solvent removal followed by crystallization of the residue from dichloromethane/ether afforded the product as 345 mg (38%) of black crystals. ^{1}H NMR (CD_3CN, anion): δ −2.85 (9), 3.84 (27), 7.52 (3), 11.63 (18), 26.8 (br, 9). Anal. Calcd for $C_{57}H_{87}B_2Fe_3N_6P_3S_4W{\cdot}CH_2Cl_2$: C, 45.37; H, 5.84; N, 5.47. Found: C, 45.89; H, 5.84; N, 5.79.

$[(Tp^*)WFe_3S_3Se(PEt_3)_3](BPh_4)$. To a stirred solution of 837 mg (0.79 mmol) of $(Et_4N)[(Tp^*)WFe_3S_3SeCl_3]$ in 50 mL of acetonitrile was added 465 mg (3.94 mmol) of PEt_3. After 1 min, a solution of 1.57 g (4.60 mmol) of $NaBPh_4$ in 8 mL of acetonitrile was introduced. The black solution was stirred for 24 h, and 170 mL of ether was added. The mixture was stirred for 5 h and filtered. The filtrate was reduced to dryness, and the residue was extracted with dichloromethane and benzene. Solvent removal followed by crystallization of the residue from acetonitrile/ether gave the product as 550 mg (47%) of black crystals. ^{1}H NMR (CD_3CN): δ −3.37 (9), 5.41 (27), 6.36 (3), 11.76 (18), 24.5 (br, 9). Anal. Calcd for $C_{57}H_{87}B_2Fe_3N_6P_3S_3SeW$: C, 45.72; H, 5.86; N, 5.61. Found: C, 45.81; H, 5.81; N, 5.43.

C. Edge-Bridged Double Cubanes. *$[(Tp^*)_2W_2Fe_6S_8(PEt_3)_4]$.* A solution of 317 mg (0.22 mmol) of $[(Tp^*)WFe_3S_4(PEt_3)_3](BPh_4)$ in 1.5 mL of acetonitrile was added to a solution of 67 mg (0.26 mmol) of $(Bu_4N)(BH_4)$ in 0.3 mL of acetonitrile. The reaction mixture was allowed to stand for 48 h. The solid that separated was collected and washed with acetonitrile to afford the product as 156 mg (70%) of a sparingly soluble black crystalline solid. This method led to much higher yields than that reported earlier, whose product was shown to be an EBDC by a structure determination.[22]

$[(Tp^*)_2W_2Fe_6S_6Se_2(PEt_3)_4]$. A solution of 300 mg (0.20 mmol) of $[(Tp^*)WFe_3S_3Se(PEt_3)_3](BPh_4)$ in 1 mL of acetonitrile was added to a solution of 62 mg (0.24 mmol) of $(Bu_4N)(BH_4)$ in 0.3 mL of acetonitrile. The preceding method gave the product as 140 mg (65%) of a sparingly soluble black crystalline solid suitable for X-ray crystallography.

D. P^N-Type Clusters. *$(Et_4N)_3[(Tp^*)_2W_2Fe_6S_7Se_2(SH)_2]$.* To a suspension of 50 mg (0.024 mmol) of $[(Tp^*)_2W_2Fe_6S_6Se_2(PEt_3)_4]$ in 20 mL of acetonitrile was added 13 mg (0.083 mmol) of $(Et_4N)(SH)$. The black solution was stirred for 48 h and filtered. Slow diffusion of ether into the filtrate resulted in the separation of a crystalline solid, which was recrystallized from acetonitrile/ether to give the product as 32 mg (64%) of black blocklike crystals. ^{1}H NMR (CD_3CN): δ −1.22 (3), −0.18 (3), −0.08 (3), 0.22 (3), 1.89 (3), 4.47 (1), 4.68 (1), 5.85 (br, 1), 7.07 (1), 28.3 (br, 3). Anal. Calcd for $C_{54}H_{106}B_2Fe_6N_{15}S_9Se_2W_2{\cdot}2CH_3CN{\cdot}(C_2H_5)_2O$: C, 32.48; H, 5.36; N, 10.39. Found: C, 32.71; H, 5.25; N, 10.30.

$(Et_4N)_3[(Tp^*)_2W_2Fe_6S_6Se_3(SeH)_2]$. $[(Tp^*)_2W_2Fe_6S_6Se_2(PEt_3)_4]$ (30 mg, 0.014 mmol) was suspended in 20 mL of acetonitrile, and a

dx.doi.org/10.1021/ja3010539 | J. Am. Chem. Soc. 2012, 134, 6479−6490

solution of 13 mg (0.062 mmol) of $(Et_4N)(SeH)$ was added, causing the solid to dissolve over 8 h. The dark-brown reaction mixture was stirred for 30 h and filtered. Slow diffusion of ether into the filtrate resulted in the separation of a crystalline solid, which was recrystallized from acetonitrile/ether to afford the product as 19 mg (59%) of black blocklike crystals. ^{1}H NMR (CD_3CN): δ −0.10 (6), 0.74 (6), 1.77 (3), 4.76 (2), 5.8 (br), 6.66 (1), 23.4 (3). Anal. Calcd for $C_{54}H_{106}B_2Fe_6N_{15}S_6Se_5W_2{\cdot}CH_3CN{\cdot}(C_2H_5)_2O$: C, 30.12; H, 5.01; N, 9.37. Found: C, 29.88; H, 4.86; N, 9.09.

$(Et_4N)_3[(Tp^*)_2W_2Fe_6S_6Se_2(SMe)_3]$. A mixture of 4.0 mg (0.060 mmol) of NaSMe and 9.0 mg (0.060 mmol) of Et_4NCl in 2 mL of acetonitrile was stirred for 24 h and then transferred into a suspension of 32 mg (0.015 mmol) of $[(Tp^*)_2W_2Fe_6S_6Se_2(PEt_3)_4]$ in 1 mL of acetonitrile. The reaction mixture was stirred for 24 h and filtered. Diffusion of ether into the filtrate gave the product as 17 mg (51%) of black blocklike crystals. ^{1}H NMR (CD_3CN): δ 0.45 (6), 0.52 (6), 0.73 (6), 4.73 (2), 4.89 (2), 5.29 (2), 34.6−35.5 (vbr, ∼9). Anal. Calcd for $C_{57}H_{113}B_2Fe_6N_{15}S_9Se_2W_2{\cdot}CH_3CN$: C, 31.91; H, 5.27; N, 10.09. Found: C, 32.09; H, 5.23; 10.19.

E. Double-Cuboidal Clusters. *$(Et_4N)[(Tp^*)_2W_2Fe_4S_9]$.* To a solution of 320 mg (2.0 mmol) of $(Et_4N)(SH)$ in 10 mL of acetonitrile was added a solution of 250 mg (2.0 mmol) of $FeCl_2$ in methanol, producing a black precipitate. This material was added to a solution of 710 mg (1.0 mmol) of $(Et_4N)[(Tp^*)WS_3]$ in 50 mL of acetonitrile. To the reaction mixture was added 1.6 g (16 mmol) of neat Et_3N under vigorous stirring, which was continued for 24 h. The black precipitate was washed with ether, dried, and recrystallized from DMF/ether to give 420 mg (52%) of black crystalline product. ^{1}H NMR (Me_2SO-d_6): δ 0.33 (3), 2.01 (3), 2.10 (6), 4.51 (6), 5.50 (2), 5.85 (1), 6.71 (1). Anal. Calcd for $C_{38}H_{64}B_2Fe_4N_{13}S_9W_2{\cdot}2C_3H_7NO$ (DMF solvate): C, 30.19; H, 4.49; N, 12.00. Found: C, 30.12; H, 4.42; N, 11.83.

$(Et_4N)_2[(Tp^*)_2W_2Fe_4S_9]$. $(Et_4N)[(Tp^*)_2W_2Fe_4S_9]$ (400 mg, 0.25 mmol) and 73 mg (0.50 mmol) of $(Et_4N)(BH_4)$ were stirred in 50 mL of acetonitrile for 12 h. The reaction mixture was filtered, and the filtrate was reduced to 30 mL and layered over 150 mL of THF. A black crystalline material was collected, washed with THF and ether, and dried, giving 338 mg (78%) of product. Crystalline product was obtained by ether diffusion into a DMF solution. ^{1}H NMR (CD_3CN): δ 1.2 (vbr, sh), 2.14 (3), 2.16 (6), 3.2 (vbr), 5.08 (vbr), 5.33 (2), 6.26 (1). Anal. Calcd for $C_{46}H_{84}B_2Fe_4N_{14}S_9W_2{\cdot}2.5C_3H_7NO$ (DMF solvate): C, 33.52; H, 5.34; N, 12.05. Found: C, 33.92; H, 5.41; N, 12.37.

$[(Tp^*)_2W_2Fe_4S_6Se_3]$. To a solution of 900 mg (1.27 mmol) of $(Et_4N)[(Tp^*)WS_3]$ in 150 mL of acetonitrile was added 518 mg (4.07 mmol) of $FeCl_2$ in 30 mL of THF. After 3 min, 322 mg (2.54 mmol) of Na_2Se in 30 mL of THF was introduced. The black reaction mixture was stirred for 30 h, and a dark-brown solid was collected. This material was recrystallized from DMF/ether to give the product as 329 mg (32%) of black blocklike crystals. ^{1}H NMR (Me_2SO-d_6): δ −0.46 (3), 1.68 (3), 1.85 (6), 5.34 (2), 5.90 (vbr), 6.60 (1). Anal. Calcd for $C_{30}H_{44}B_2Fe_4N_{12}S_6Se_3W_2C_3H_7NO{\cdot}(C_2H_5)_2O$: C, 25.22; H, 3.49; N, 10.33. Found: C, 25.05; H, 3.64; N, 10.69.

$(Et_4N)_2[(Tp^*)_2W_2Fe_4S_6Se_3]$. To a solution of 100 mg (0.12 mmol) of $(Et_4N)[(Tp^*)WFeS_3Cl_2]$ in 5 mL of acetonitrile was added a slurry of 15 mg (0.12 mmol) of $FeCl_2$ in 5 mL of THF. After 2 min, a suspension of 30 mg (0.24 mmol) of Na_2Se in 5 mL of THF was introduced. The black reaction mixture was stirred for 1 day. A dark-brown precipitate was collected and crystallized from DMF/ether to afford the product as 48 mg (43%) of black blocklike crystals. ^{1}H NMR (Me_2SO-d_6): δ 0.85 (vbr), 5.02 (br), 5.34 (2), 6.35 (1).

In the sections that follow, clusters are designated numerically according to Chart 1. For simplicity in the X-ray section, compounds are referenced by their cluster numbers.

X-ray Structure Determinations. The structures of the 14 compounds in Table S1 in the Supporting Information were determined. Diffraction-quality crystals of **2**−**4**, **5b**, and **7b** were obtained by ether diffusion into acetonitrile solutions. Crystalline **6b** was acquired by ether diffusion into a THF solution, and crystals of **9**−**15** were grown by ether diffusion into DMF solutions. Data were collected on a Bruker APEX II CCD diffractometer equipped with an Oxford Cryostream 700 series low-temperature apparatus operating at 100 K. Raw data were integrated and corrected for Lorentz and polarization effects using the Bruker APEX II program suite. Absorption corrections were applied using SADABS. Space groups were assigned by analysis of symmetry and systematic absences (as determined by XPREP) and were further checked by PLATON. Structures were solved by direct methods and refined against all data in the 2θ ranges by full-matrix least-squares on F^2 with the SHELXL program suite using the OLEX 2 interface. Hydrogen atoms at idealized positions were included in the final refinements. The OLEX 2 interface was also used for structure visualization and drawing ORTEP figures.

Chart 1. Designations of Clusters and Ligands

$[(Tp^*)WS_3]^{1-}$	**1**[21]
$[(Tp^*)WFeS_3Cl_2]^{1-}$	**2**
$[(Tp^*)WFe_2S_3(SEt)Cl_2]^{1-}$	**3**
$[(Tp^*)WFe_2S_3(SEt)_3]^{1-}$	**4**
$[(Tp^*)WFe_3S_3QCl_3]^{1-}$	Q = S, **5a**;[22] Q = Se, **5b**
$[(Tp^*)WFe_3S_3Q(SEt)_3]^{1-}$	Q = S, **6a**;[22] Q = Se, **6b**
$[(Tp^*)WFe_3S_3Q(PEt_3)_3]^{1+}$	Q = S, **7a**; Q = Se, **7b**
$[(Tp^*)_2W_2Fe_6S_6Q_2(PEt_3)_4]$	Q = S, **8a**; Q = Se, **8b**
$[(Tp^*)_2W_2Fe_6S_7Se_2(SH)_2]^{3-}$	**9**
$[(Tp^*)_2W_2Fe_6S_6Se_3(SeH)_2]^{3-}$	**10**
$[(Tp^*)_2W_2Fe_6S_6Se_2(SMe)_3]^{3-}$	**11**
$[(Tp^*)_2W_2Fe_4S_9]^{1-}$	**12**
$[(Tp^*)_2W_2Fe_4S_9]^{2-}$	**13**
$[(Tp^*)_2W_2Fe_4S_6Se_3]$	**14**
$[(Tp^*)_2W_2Fe_4S_6Se_3]^{2-}$	**15**
1,3,5-*tert*-butyl-1,3,5-triazacyclohexane	Bu^t_3tach
ethane-1,2-dithiolate(2−)	edt
tris(pyrazolyl)hydroborate(1−)	Tp
tris(3,5-dimethylpyrazolyl)hydroborate(1−)	Tp*

For selenium-containing compounds, all non-hydrogen atoms were located in difference Fourier maps. Careful refinement results clearly showed the varying S/Se populations at μ_2 sites in **9** and **11**, indicating that other sites assigned to selenium in these and other clusters are fully occupied. Refined bond lengths at these sites further support selenium occupation. Constraints of both the positions and displacement parameters (using the EXYZ and EADP instructions in SHELXL-97) as well as constraints of the S−CH_3 bond length in **11** (using the SADI instructions in SHELXL-97) were applied to the disorder refinements. The occupancy ratios of the two μ_2-S/Se sites in **9** derived from the refinements were 0.481(5)/0.519(5) and 0.567(4)/0.433(4). In the final refinement, a 1:1 ratio was used. A similar procedure was applied to the two μ_2-S/Se sites in **11**.

Other Physical Measurements. ^{1}H NMR spectra were obtained with a Varian M400 spectrometer. ^{57}Fe Mössbauer spectra were measured with a constant-acceleration spectrometer. Data were analyzed with Igor Pro 6 software (Wavemetrics, Portland, OR); isomer shifts are referenced to iron metal at room temperature. Cyclic voltammetry measurements were made with a BioAnalytical Systems Epsilon potentiostat/galvanostat in DMF or acetonitrile solutions at 100 mV/s using a glassy carbon working electrode, 0.1 M $(Bu_4N)(PF_6)$ as the supporting electrolyte, and an SCE reference electrode.

RESULTS AND DISCUSSION

This research has two primary goals: (i) exploration of the concept of template-assisted cluster assembly and (ii) determination of the structural fate of sulfide or selenide, introduced as free reactants (external) or bound in cluster precursors (internal), in cluster

dx.doi.org/10.1021/ja3010539 | J. Am. Chem. Soc. 2012, 134, 6479−6490

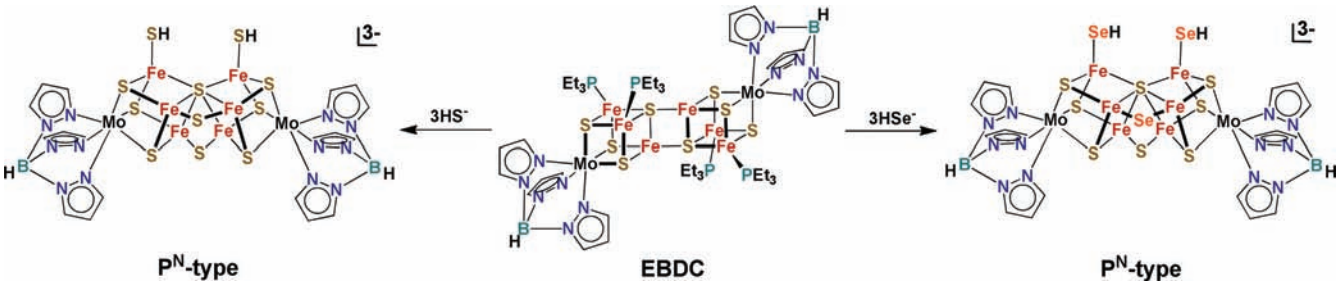

Figure 1. Depiction of the conversion of the EBDC cluster $[(Tp)_2Mo_2Fe_6S_8(PEt_3)_4]$ to P^N-type clusters by reactions with HQ^- (Q = S, Se) in acetonitrile. The μ_2 position of selenide in the product cluster should be noted.

formation. In (i), we employed as the template $[(Tp^*)W^{VI}S_3]^{1-}$, the entirety of which in a reduced form was intended to be a component of the final product. Summarized in Figure 1 is the only previous attempt to address (ii). Cluster conversion reaction 1[23] proceeds by reaction of hydrosulfide (Q = S) with an EBDC to yield a P^N-type cluster whose most distinctive feature is a μ_6-S atom with one large Fe−(μ_6-S)−Fe external angle that is present in a core topologically equivalent to that of the P^N cluster of nitrogenase (see below).[15,24,25] The structural fate of the attacking nucleophile was decided by the use of hydroselenide (Q = Se), which afforded a product containing selenide only in a doubly bridging position, as determined by an X-ray structure.[17]

$$[(Tp)_2Mo_2Fe_6S_8(PEt_3)_4] + 3HQ^- \rightarrow [(Tp)_2Mo_2Fe_6S_8Q(QH)_2]^{3-} + 4PEt_3 + \frac{1}{2}H_2 \quad (1)$$

In the present context, the choice of selenide as a surrogate for sulfide was predicated on the small differences in their ionic radii ($r_{Se^{2-}} - r_{S^{2-}}$ = 1.91 Å − 1.84 Å = 0.07 Å) and covalent radii ($r_{Se} - r_S$ = 1.17 Å − 1.04 Å = 0.13 Å)[26] and the slightly smaller bond angles at selenium always found in comparative molecules in which only the chalcogenide atom (Q = S or Se) is varied. Also, replacement of sulfide by selenide in general produces only a small positive shift (often ≤50 mV) in redox potentials. These factors contribute to the existence of a sizable body of analogous stable clusters with selenide or sulfide core atoms[27] and clusters with sulfur and selenium in the same cubane core $[Fe_4S_{4-n}Se_n]^{2+/1+}$ (n = 1−3).[28] Prominent examples of the latter type are found with the cubane pair $[Fe_4Q_4(SPh)_4]^{2-}$ (Q = S, Se)[29] whose members are isostructural but not exactly isometric. Further, iron−selenide clusters comparable to native clusters have been reconstituted in ferredoxin-type proteins.[30] As will be seen, S/Se substitution is possible in the core units of five clusters having different structures.

Cluster Syntheses and Structures. The syntheses of five types of W−Fe−S/Se clusters are described in the sections that follow. Feasible reaction stoichiometries are indicated; non-cluster reaction products were not identified. Cluster yields refer to the isolated Et_4N^+ salts. Synthetic schemes are set out in Figures 2, 5, and 8 and X-ray structures in Figures 3, 4, 6, 7, and 10. Detailed structural descriptions of the clusters are not required for the purpose of this work; metric data are given in the Supporting Information.[31] The Mössbauer spectra usually consisted of a single quadrupole doublet or less frequently two overlapping doublets. Oxidation states (s) were obtained from the ^{57}Fe isomer shifts (δ) using the empirical relationship δ = 1.43 − 0.40s, which is best applied at and above 77 K[32] to tetrahedral FeS_4 sites with anionic ligands. The values δ = 0.63 and 0.23 mm/s were estimated for Fe^{2+} and Fe^{3+}, respectively. This relationship can also be applied, although less accurately, to FeS_3L sites with one non-sulfur ligand. At constant oxidation state, isomer shifts generally tend to decrease in the order $Cl^- > RS^- > R_3P$.[33] Mössbauer parameters from zero-field spectra are collected in Table 1. Iron oxidation states are written as $Fe^{2+/3+}$, but as for nearly all Fe−S and M−Fe−S weak-field clusters, the electronic structures are actually delocalized. Tungsten oxidation states were obtained by difference and are confined to $W^{3+/4+}$ because of limits on the iron oxidation states and experimental cluster charges. Oxidation state formalisms are useful in following redox changes in synthetic reactions. The stated values are sensibly consistent with isomer shift data but cannot be considered as demonstrated. Also collected in Table 1 are redox potentials for chemically reversible processes ($i_{pc}/i_{pa} \approx 1$).

Table 1. Zero-Field Mössbauer Parameters (δ and ΔE_Q) and Redox Potentials ($\Delta E_{1/2}$)

cluster	δ (mm/s)[a]	ΔE_Q (mm/s)	$\Delta E_{1/2}$ (V)[b]
2	0.52	1.17	irrev
4	0.45	1.02	−0.17 (1−/2−), −1.42 (2−/3−)
5a	0.50	0.86	−0.72 (1−/2−), −1.69 (E_{pc})[c]
5b	0.52	0.96	-0.69 (1−/2−), −1.64 (E_{pc})[c]
6a	0.42	1.41	−1.13 (1−/2−), −2.12 (E_{pc})
6b	0.44	1.27	−1.10 (1−/2−), −1.92 (2−/3−)
7a	0.49[d]	*e*	−0.96 (1+/0)
7b	0.51[d]	*f*	−0.89 (1+/0)
8a	0.61	0.84	n.d.[g]
8b	0.61	0.84	n.d.[g]
9	0.55[d]	*h*	−1.19 (2−/3−), −1.83 (3−/4−)
10	0.57[d]	*k*	n.d.[g]
11	0.62	0.81	−0.85 (1−/2−), −1.39 (2−/3−)
12[i]	0.37	1.21	−0.54 (1−/2−), −1.99 (2−/3−), −2.40 (3−/4−)
13[i]	0.42	0.98	−0.54 (1−/2−), −1.97 (2−/3−), −2.38 (3−/4−)
14	0.41	1.21	—
15[i]	0.43	1.15	−0.51 (1−/2−), −1.91 (2−/3−), −2.19 (3−/4−)[j]

[a] 90−120 K, vs Fe metal at room temperature. [b] V vs SCE, 298 K, acetonitrile, unless noted otherwise. [c] Peak potential, irreversible. [d] Weighted mean value of two overlapping doublets. [e] ΔE_Q = 0.84 (71%), 2.28 (29%). [f] ΔE_Q = 0.87 (72%), 1.78 (28%). [g] Not determined. [h] ΔE_Q = 0.77 (61%), 0.93 (39%). [i] Potentials in DMF. [j] Approximate value. [k] ΔE_Q = 0.66 (71%), 1.12 (29%).

1. Incomplete Cubane Clusters. The syntheses of the clusters of all types originated with the mononuclear W^{VI} template complex **1**. Relatively simple products are derivable from

dx.doi.org/10.1021/ja3010539 | J. Am. Chem. Soc. 2012, 134, 6479−6490

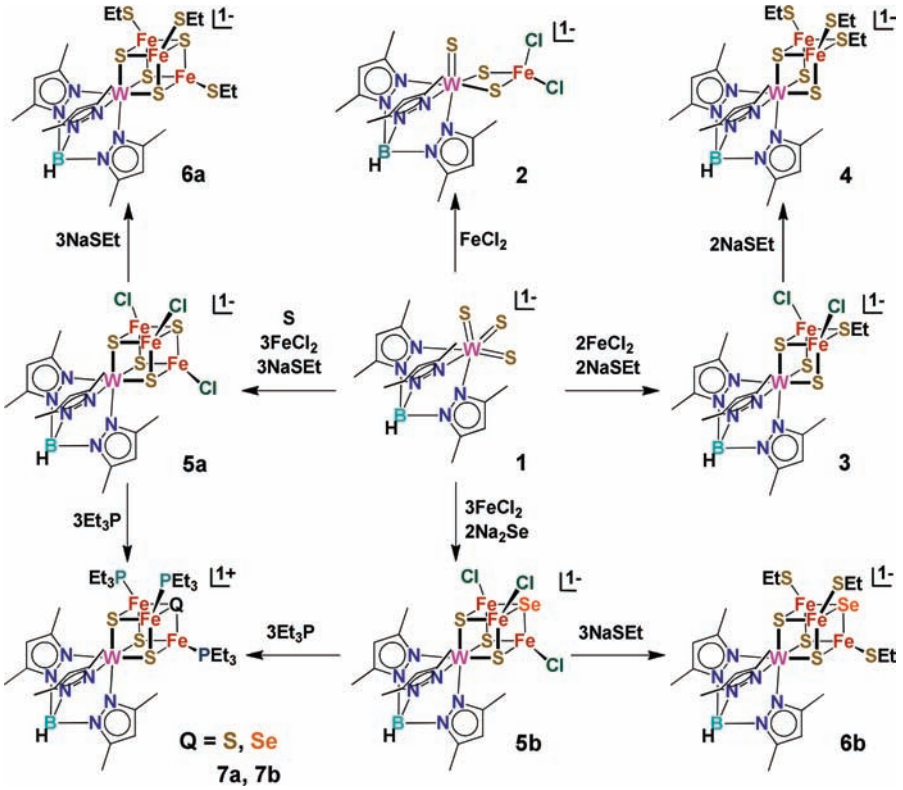

Figure 2. Synthetic scheme for incomplete cubanes **2**–**4** and cubane-type clusters **5a** and **5b** from template precursor **1**. Clusters **6ab** and **7ab** are obtained from **5a** and **5b** by ligand substitution reactions.

it using 1 or 2 equiv of $FeCl_2$ according to reactions 2–4, as shown in Figure 2; the structures of the products **2**–**4** are shown in Figure 3. Reaction 2 is not a redox process. Addition of 1 equiv of $FeCl_2$ to **1** affords binuclear **2** (84%) with six-coordinate W^{VI} and tetrahedral Fe^{II}. The η^2 binding mode of the WS_3 group has been observed previously with the heavier metals of groups 8–10.[21] The dimensions of the WS_2Fe rhombus are nearly the same as in related molecules such as $[S_2WS_2FeX_2]^{2-}$(X = anion)[34−36] and $[(Me_2PCH_2CH_2S)W(S)S_2FeCl_2]^{1-}$.[37] The product is best considered as $W^{6+}Fe^{2+}$, with the isomer shift of 0.52 mm/s relative to an FeS_4 site apparently decreased by some extent of electron delocalization to the fully oxidized tungsten site. Reaction with 2 equiv each of $FeCl_2$ and NaSEt produces trinuclear **3**[38] (61%), which undergoes ligand substitution reaction 4 to yield isostructural **4** (49%), whose isomer shift of 0.45 mm/s suggests the description $W^{4+}Fe^{3+}Fe^{2+}$. Consequently, Fe^{2+} and EtS^- are reductants of W^{6+} in reaction 3. Cluster **4** sustains a three-member electron transfer series; if the charge distribution is correct, the first reduction is likely to be iron-based and the second reduction at tungsten. The incomplete cubane description of **3** and **4** is evident from a vacancy at the site where an iron atom might be bound and by inclusion of a bridging ethanethiolate at a sulfide site. These clusters are apparently trapped intermediates in cluster assembly. Formation of the thiolate bridge positions an ethyl group in front of the iron site (Fe−S−C angles of 106° and 109° in **4**), a possible impediment to completion of the cubane core. As will be seen, the WFe_2S_3 portions of **3** and **4** are present in higher-nuclearity clusters.

$$[(Tp^*)WS_3]^{1-} + FeCl_2 \rightarrow [(Tp^*)WFeS_3Cl_2]^{1-} \quad (2)$$

$$[(Tp^*)WS_3]^{1-} + 2FeCl_2 + 2NaSEt \rightarrow [(Tp^*)WFe_2S_3Cl_2(SEt)]^{1-} + \frac{1}{2}EtSSEt + 2NaCl \quad (3)$$

$$[(Tp^*)WFe_2S_3Cl_2(SEt)]^{1-} + 2NaSEt \rightarrow [(Tp^*)WFe_2S_3(SEt)_3]^{1-} + 2NaCl \quad (4)$$

2. Single Cubane Clusters. Synthetic methods are summarized in Figure 2. Cluster **5a** was prepared previously from the assembly system **1**/3$FeCl_2$/S/3NaSEt utilizing a four-electron reduction of **1** and sulfur; cubane **6a** was prepared by ligand substitution.[22] Cluster **5b** (64%) was obtained here by the related reaction 5 using selenide as a ligand and probable reductant. It was also prepared from the system **2**/3$FeCl_2$/2Na_2Se in 77% yield. Reaction 6 yielded the thiolate cluster **6b** (61%). The isomer shifts of the pairs **5a**/**5b** and **6a**/**6b** follow the order Cl^- > EtS^- (Table 1), as do those of $[(Tp)MoFe_3S_4L_3]^{1-}$ (L = Cl^-, 0.49 mm/s; L = EtS^-, 0.39 mm/s)[39] with very similar shifts. For **6a** and **6b**, the shifts of 0.42 and 0.44 mm/s are intermediate between the estimates of 0.36 mm/s for $W^{3+}Fe^{2+}Fe^{3+}{}_2$ and 0.50 mm/s for $W^{4+}Fe^{2+}{}_2Fe^{3+}$. We favor the former description for **5a**/**5b** and **6a**/**6b** on the basis of our analysis of $[(Tp)MoFe_3S_4Cl_3]^{1-}$ and the likelihood that the core charge distribution with chloride and thiolate terminal ligands will not change appreciably. In this case, the reduction steps (Table 1) would be iron-based, and Fe^{II} and selenide are reductants of W^{VI} in reaction 5. Clusters **7a** (38%) and **7b** (47%) are accessible by chloride substitution of **5a** and **5b**, respectively, with excess phosphine. One-electron cluster reduction by phosphine to give the $[MoFe_3S_4]^{2+}$ oxidation level is precedented.[15,40] The Mössbauer spectra consist of two

dx.doi.org/10.1021/ja3010539 | J. Am. Chem. Soc. 2012, 134, 6479–6490

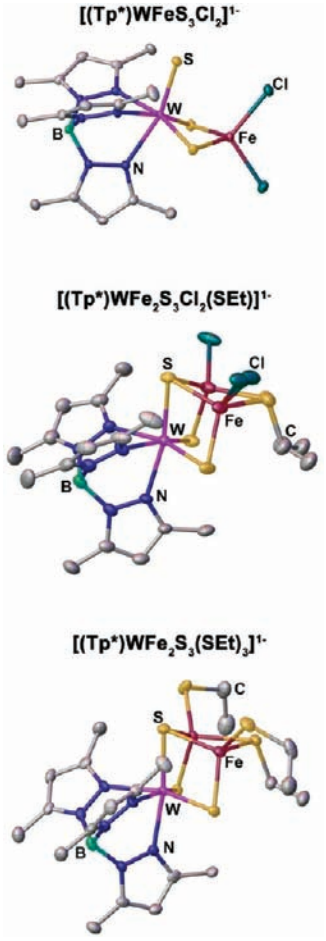

Figure 3. Structures of the incomplete cubane clusters **2**–**4**. In this and succeeding figures, 50% probability ellipsoids are shown. Disorder in the chloride ligands of **3** is evident. Selected dimensions (Å, deg) in **2**: W═S, 2.159(1); W–S, 2.292(2); Fe–S, 2.255(1); W–Fe, 2.724(1); S–Fe–S, 102.83(3).

overlapping quadrupole doublets. The mean isomer shifts are suggestive of the description $W^{3+}Fe^{2+}{}_2Fe^{3+}$. An analogous description has been deduced for $[MoFe_3S_4]^{2+}$ clusters.[40,41]

$$[(Tp^*)WS_3]^{1-} + 3FeCl_2 + 2Na_2Se \rightarrow [(Tp^*)WFe_3S_3SeCl_3]^{1-} + 3NaCl + \frac{1}{2}Na_2Se_2 \quad (5)$$

$$[(Tp^*)WFe_3S_3SeCl_3]^{1-} + 3NaSEt \rightarrow [(Tp^*)WFe_3S_3Se(SEt)_3]^{1-} + 3NaCl \quad (6)$$

The structures of **5b** and **6b** (Figure 4) and **7b** (Figure 6) demonstrate the specific incorporation of selenide into the cluster cores, whose structures respond to the incorporation of that atom. In selenide cluster **6b**, for example, the mean Fe–Se bond length and Fe–Se–Fe bond angle are 2.37(2) Å and 68.8°, respectively, whereas in **6a**,[22] the corresponding values at the same site are 2.25(3) Å and 72.6°. As shown in Table 2, the same trend in bond lengths and angles holds for corresponding S/Se sites in all of the other clusters. It should be noted also that the recent isolation of the cluster $[Fe_4S_3(NBu^t)Cl_3]^{2-}$ (Fe–N 1.95 Å)[42] is a further indication of the structural

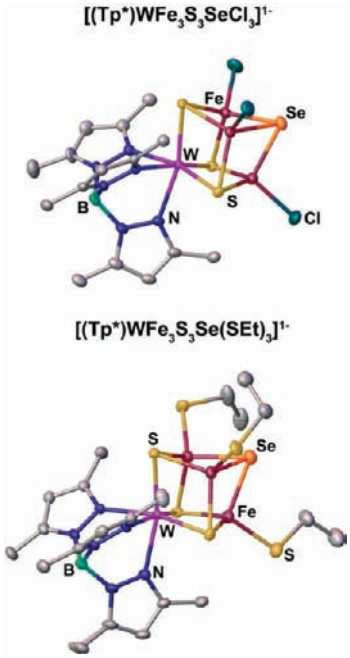

Figure 4. Structures of the cubane-type clusters **5b** and **6b** revealing the specific incorporation of a μ_3-Se atom in their cores.

Table 2. Dimensional Comparison of Fe–Q Cluster Fragments[a]

fragment	cluster	Distances (Å)	angles (°)
Fe—QH[b]	**9** (Q=S)	2.322(2)	—
	10 (Q=Se)	2.448(1)	—
Fe Q Fe	**13** (Q=S)[c]	2.23(1)	76.7(1)
			75.05(7)
	15 (Q=Se)[c]	2.364(9)	
	$[(Tp)_2Mo_2Fe_6S_9(SH)_2]^{3-}$[d]	2.225(5)	75.0(4)
	10 (Q=Se)[e]	2.375(7)	77.0(5)
Fe Fe Q Fe	**5a**[f]	2.259(5)	73.2(2)
	5b[f]	2.39(1)	68.9(6)
Fe a Q b Q Fe	**8a** (Q=S)[g]	(a)2.290(2)	78.22(6)
		(b) 2.393(2)	
	8b (Q=Se)[g]	(a) 2.388(1)	77.08(3)
		(b) 2.510(1)	
Fe Fe Q Fe Fe	**13** (Q=S)[c]	2.32(1)[h]	68.4(1)
			73.3(6)
			110(1)
	15 (Q=Se)[c]	2.461(2)[h]	64.9(4)
			71.7(4)
			105(1)
Fe Fe Fe Q Fe Fe	$[(Tp)_2Mo_2Fe_6S_9(SH)_2]^{3-}$[d]	2.38(2)[i]	70.3(5)[i]
			68.9(5)[i]
			108(2)[i]
	10 (Q=Se)[e]	2.51(3)[i]	65(2)[i]
			71.7(4)[j]
			104(2)[j]

[a]Mean values are used where possible. [b]Terminal bond. [c]Double-cuboidal. [d]See ref 15. [e]P^N-type. [f]Cubane-type. [g]EBDC. [h]Mean value of four values. [i]Mean value of six values. [j]Mean value of two values.

dx.doi.org/10.1021/ja3010539 | J. Am. Chem. Soc. 2012, 134, 6479–6490

flexibility of weak-field cubane clusters, which allows them to accommodate bridging atoms having very different radii.

3. Edge-Bridged Double Cubanes. Borohydride reduction of **7a** and **7b** (reaction 7) afforded the sparingly soluble EBDCs **8a** (Q = S, 70%) and **8b** (Q = Se, 65%,). The **7b** → **8b** reaction is illustrated in Figure 5, and the structures of these clusters are

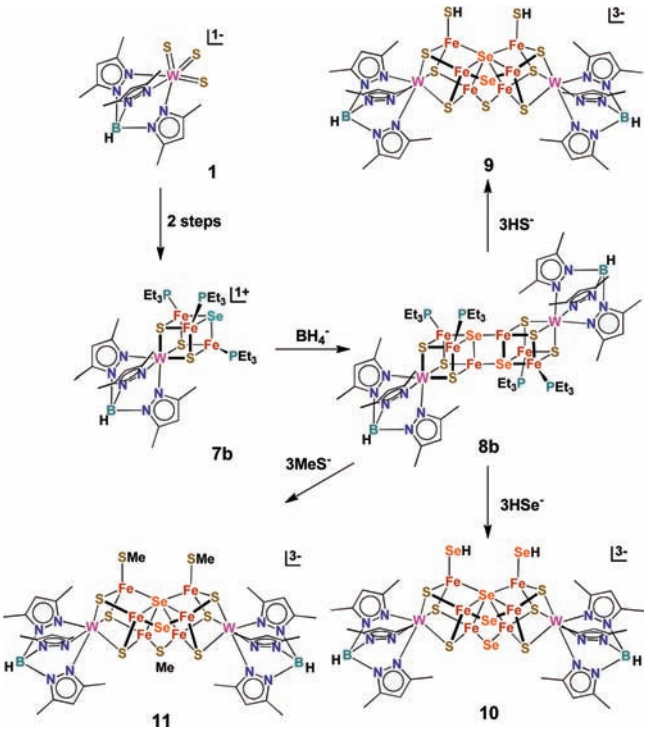

Figure 5. Synthetic scheme for the reduction of single-cubane **7b** to give diselenide EBDC cluster **8b** and the conversion of **8b** to P^N-type clusters **9**–**11** by reaction with sulfide or selenide nucleophiles.

presented in Figure 6. An analogous reaction series leading to $[(Tp)_2Mo_2Fe_6S_8(PEt_3)_4]$ was described previously.[15−17] Clusters **8a** and **8b** contain $[W_2Fe_6S_6Q_2]^{2+}$ cores whose identical isomer shifts (0.61 mm/s) and electron counts lead to the all-ferrous formulation $W^{3+}{}_2Fe^{2+}{}_6$.

$$2[(Tp^*)WFe_3S_3Q(PEt_3)_3]^{1+} + 2BH_4^- \rightarrow [(Tp^*)_2W_2Fe_6S_6Q_2(PEt_3)_4] + 2PEt_3 + H_2 + B_2H_6 \quad (7)$$

Dimerization of the $[MFe_3S_4]$ core can in principle generate six EBDC isomers of $[M_2Fe_6S_8]$, two with centrosymmetry and four others that constitute enantiomeric pairs.[31] All EBDCs whose structures are known have a real or idealized centrosymmetric structure with an $Fe_2(\mu_4\text{-}S)_2$ bridging rhombus and heterometal atoms in distant transoid positions (Figure 1). Cluster **8b** adheres to this regularity, having crystallographically imposed centrosymmetry with the μ_3-Se atoms in reactant **7b** occupying the two μ_4-Q positions of an EBDC.

4. P^N-Type Clusters. The prototypical molybdenum cluster of this type, $[(Tp)_2Mo_2Fe_6S_9(SH)_2]^{3-}$, is formed by reaction 1 (Q = S). Given the results in Figure 1, a corresponding experiment with tungsten clusters is unnecessary inasmuch as the same outcome is entirely probable. Here we consider the reactions of the diselenide EBDC **8b** with 3 equiv of each of three external nucleophiles (reactions 8−10), which are

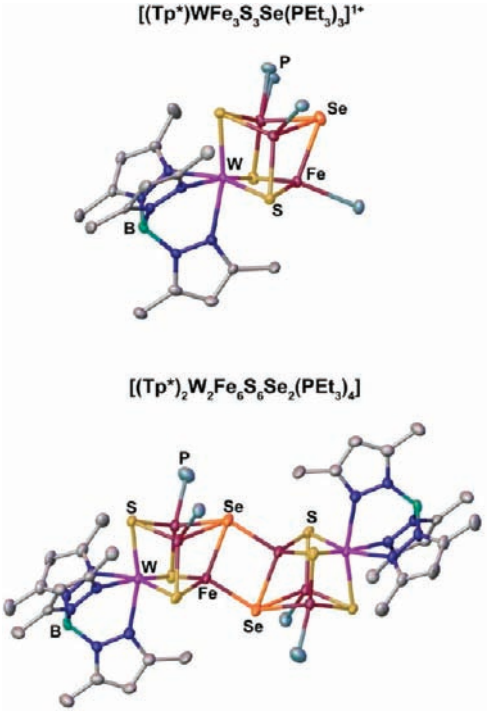

Figure 6. Structures of the cubane-type cluster **7b** and its EBDC reduction product **8b** (imposed centrosymmetry); the μ_4 positions of the two selenide atoms should be noted. Ethyl groups have been omitted for clarity. Selected distances for **8b** (Å): Fe···Fe, 3.053(3) (bridge rhombus); Se···Se, 3.832(3); W···W, 8.347(5).

illustrated in Figure 5. These reactions yield P^N-type clusters **9** (64%), **10** (59%), and **11** (51%), whose structures are shown in Figure 7. The isomer shifts of **9** (0.55 mm/s), **10** (0.57 mm/s), and **11** (0.62 mm/s) indicate reduced oxidation levels. The $[W_2Fe_6S_7Se_2]^{1+}$ core of **9** and the $[W_2Fe_6S_6Se_3]^{1+}$core of **10** are formulated as $W^{3+}{}_2Fe^{2+}{}_5Fe^{3+}$, and the $[W_2Fe_6S_6Se_2(SMe)]^{1+}$ core of **11** is formulated as $W^{3+}{}_2Fe^{2+}{}_6$, consistent with the larger isomer shift of the latter. The core units are built from two distorted cubane units with a μ_6-Se common vertex that are further connected by μ_2-Q (**9**–**11**) and μ_2-SMe (**11**) bridges.

$$[(Tp^*)_2W_2Fe_6S_6Se_2(PEt_3)_4] + 3HS^- \rightarrow [(Tp^*)_2W_2Fe_6S_7Se_2(SH)_2]^{3-} + \frac{1}{2}H_2 + 4PEt_3 \quad (8)$$

$$[(Tp^*)_2W_2Fe_6S_6Se_2(PEt_3)_4] + 3HSe^- \rightarrow [(Tp^*)_2W_2Fe_6S_6Se_3(SeH)_2]^{3-} + \frac{1}{2}H_2 + 4PEt_3 \quad (9)$$

$$[(Tp^*)_2W_2Fe_6S_6Se_2(PEt_3)_4] + 3MeS^- \rightarrow [(Tp^*)_2W_2Fe_6S_6Se_2(SMe)_3]^{3-} + 4PEt_3 \quad (10)$$

The central part consists of an Fe_4Se rectangular pyramid with a planar base. The most characteristic features are μ_6-Se bridging atoms and large Fe−Se−Fe angles (151−160°) centered at these atoms. There was no evidence from structural data of any significant population of selenium atoms at μ_3 positions. Structural considerations for molybdenum P^N-type clusters[15,17] largely apply to the tungsten clusters.

dx.doi.org/10.1021/ja3010539 | J. Am. Chem. Soc. 2012, 134, 6479−6490

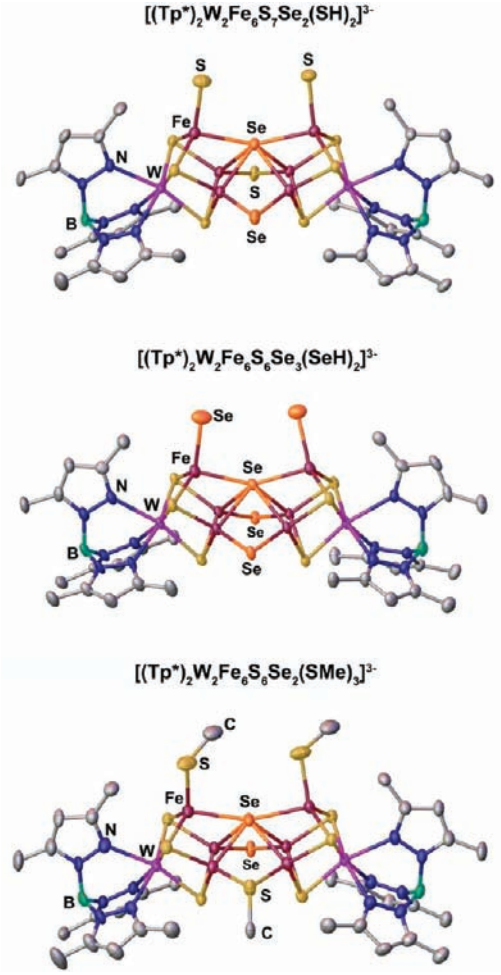

Figure 7. Structures of the P^N-type clusters **9** [155.34(4)°], **10** [150.99(5)°], and **11** [159.6(4)°], each of which contains a μ_6-Se atom. The bottom structure contains disordered Se and SMe bridges at the μ_2 positions. For clarity, a structure without disorder is depicted. The largest Fe−(μ_6-Se)−Fe angle involving Fe atoms with terminal ligands is given for each cluster.

Cluster **9** results from hydrosulfide attack and contains a μ_6-Se bridge and a μ_2-Se atom disordered over the two doubly bridging positions. The mirror symmetry in acetonitrile solution is indicated by 10 well-resolved Tp* signals in the ^{1}H NMR spectrum.[31] In the spectra of **9** and **10**, signals of coordinated QH^- were not located. Cluster **10** is formed with hydroselenide and incorporates one μ_6-Se and two μ_2-Se atoms; the remaining hydroselenides are bound in terminal positions. Cluster **11** is the product of the reaction with a nucleophile for which occupation of a μ_6 position is utterly improbable. Accordingly, one μ_2-SMe bridge is formed and is disordered over the μ_2-Se site; two methanethiolate anions are terminally bound. Reactions 8 and 9 involve a one-electron oxidation of the reactant,[23] whereas reaction 10 proceeds by addition of methanethiolate to the core with no change in isomer shift. In this reaction, the absence of a protic source and the presence of a monoanionic bridging ligand tend to stabilize the all-ferrous core. Cluster **11** is the only P^N-type cluster isolated with a monoanionic bridge component.

5. Double-Cuboidal Clusters.[43] The reaction of **1** with 2 equiv each of $FeCl_2$ and HS^- (reaction 11) yields cluster monoanion **12** (52%), which undergoes a one-electron reduction with borohydride to give dianion **13**. Isomer shifts lead to the formulations $W^{4+}{}_2Fe^{3+}{}_3Fe^{2+}$ (**12**) and $W^{4+}{}_2Fe^{3+}{}_2Fe^{2+}{}_2$ (**13**). Alternative formulations involving W^{III} ($W^{3+}W^{4+}Fe^{3+}{}_4$ for **12**, $W^{3+}W^{4+}Fe^{3+}{}_3Fe^{2+}$ for **13**) predict isomer shifts lower than those observed. In this interpretation, the formation of **12** requires a four-electron reduction of the tungsten reactant by 3 equiv of $FeCl_2$ and hydrosulfide.

$$2[(Tp^*)WS_3]^{1-} + 4FeCl_2 + 4HS^- + 4Et_3N \rightarrow [(Tp^*)_2W_2Fe_4S_9]^{1-} + 4(Et_3NH)Cl + 4Cl^- + \frac{1}{2}S_2{}^{2-} \quad (11)$$

Shown in Figure 8 is the preparative scheme for these clusters. The selenium-containing clusters **14** (32%) and **15**

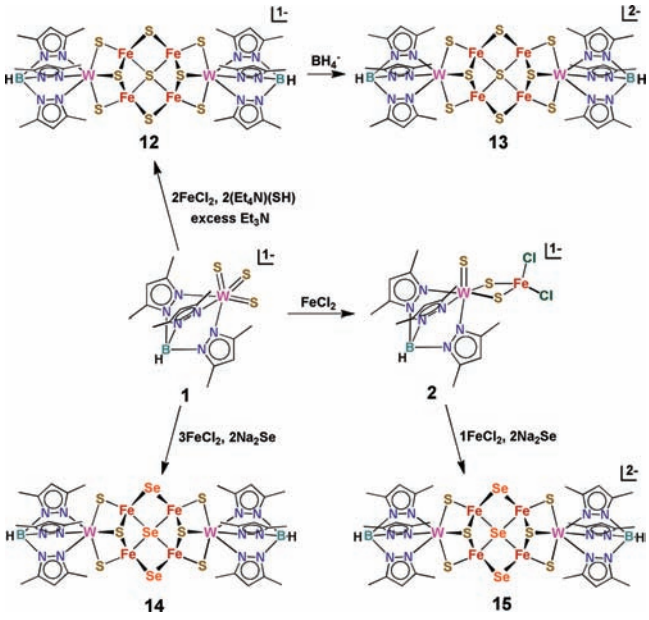

Figure 8. Synthetic scheme for double-cuboidal clusters **12**−**15** based on the reactions of $FeCl_2$ and sulfide or selenide with **1** or **2**.

(43%) are accessible in moderate yields by reactions 12 and 13, respectively. The isoelectronic relationship between dianions **13** and **15** is apparent from the pairs of sharp signals at 5.3−6.4 ppm. Cluster synthesis proves the existence of three oxidation states. The voltammograms of **13** and **15** (Figure 9) demonstrate the formation of two more oxidation states below −1.9 V (Table 1), thereby defining the five-member electron transfer series $[(Tp^*)_2W_2Fe_4S_6Q_3]^{0/1-/2-/3-/4-}$. The 0/1− steps for all of the clusters (not shown) and the 3−/4− step for **15** are not well-defined in the DMF medium used. We interpret the 1−/2− step (**12** + e^- ⇄ **13**) as iron-based, involving the configurations deduced from isomer shifts. We do not know the site of reaction for the last two steps but raise the possibility that they are W^{4+}/W^{3+} processes. The isomer shift orders **12** < **13** and **14** ≤ **15** are consistent with the second member of each pair being more reduced, but the shift differences of 0.05 and 0.02 mm/s, respectively, are much smaller that the value (0.63 − 0.23)/4 = 0.10 mm/s predicted from the empirical relationship. This may be a result of electron delocalization including the WS_3 groups.

$$2[(Tp^*)WS_3]^{1-} + 4FeCl_2 + 3Na_2Se \rightarrow [(Tp^*)_2W_2Fe_4S_6Se_3] + 6NaCl + 2Cl^- \quad (12)$$

dx.doi.org/10.1021/ja3010539 | J. Am. Chem. Soc. 2012, 134, 6479−6490

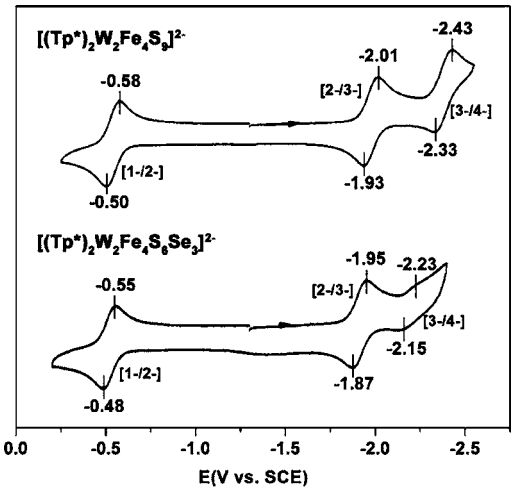

Figure 9. Cyclic voltammograms (100 mV/s) of double-cuboidal clusters **13** and **15** in DMF at ambient temperature; peak potentials are indicated.

$$2[(\mathrm{Tp^*})\mathrm{WS_3FeCl_2}]^{1-} + 2\mathrm{FeCl_2} + 4\mathrm{Na_2Se} \rightarrow [(\mathrm{Tp^*})_2\mathrm{W_2Fe_4S_6Se_3}]^{2-} + 8\mathrm{NaCl} + \mathrm{Se} \quad (13)$$

As revealed in Figure 10, the cluster structures are built upon a W_2Fe_4 plane with a nearly square Fe_4 portion. The cuboidal $WFe_2(\mu_2\text{-S})_2(\mu_3\text{-S})(\mu_4\text{-Q})$ units are recognizable by the connectivity and, as depicted for **12**, the placement of the μ_2-S and μ_4-Q atoms on one side of the plane and the μ_3-S and μ_2-Q atoms on the other. Selected metrical features are summarized in Table 3; there is no systematic trend in these bond lengths and angles with oxidation state. The $[M_2Fe_4(\mu_2\text{-Q})_6(\mu_3\text{-Q})_2(\mu_4\text{-Q})]$ connectivity pattern was first and most frequently demonstrated with $[Fe_6S_9(SR)_2]^{4-}$,[44−48] and it is also found in the selenide clusters $[Fe_6Se_9(SR)_2]^{4-}$.[49,50] The only other heterometal clusters of this type are $[(edt)_2Mo_2Fe_6S_9]^{3-/4-}$ whose cores are isoelectronic with **12** and **13** but differ by the presence of trigonal-bipyramidal molybdenum sites.[52] The isomer shift of the 4− cluster was interpreted in terms of the charge distribution $(Mo^{4+}{}_2Fe^{3+}{}_2Fe^{2+}{}_2)$, corresponding to that of **13**.

Selenide Cluster Incorporation. The conversion of an EBDC to a P^N-type cluster in reaction 1 originally provoked the issue of the fate of the attacking hydrosulfide in the formation of the $[Mo_2Fe_6S_8Q]^{1+}$ core.[17] Included in Figure 11 is the result depicted in Figure 1 in which one selenide is incorporated in a μ_2-Se site of the product core. The syntheses and structures of single cubanes, EBDCs, P^N-type clusters, and double-cuboidal clusters reveal that selenide can function as an external nucleophilic reactant when incorporated into cluster cores or as an internal, presumably intramolecular, reactant upon conversion of one cluster core to another. The situation is summarized in Figure 11. In all cases, the X-ray structural results revealed no significant selenium occupation of cluster sites other than those specified.

1. Single Cubanes. The synthesis of clusters **5b**−**7b** provides examples of the incorporation of selenide into cubane $[MFe_3S_3Q]^{3+/2+}$ cores (Figures 2 and 5). These results are consistent with the prior formation of $[(Bu^t{}_3tach)MoFe_3S_3SeL_3]^{1-/0}$ and $[(Bu^t{}_3tach)WFe_3S_3SeL_3]$ by reaction of $[(Bu^t{}_3tach)MS_3]$ with $FeCl_2$, Na_2Se, and L = Cl^- or RS^-.[5] These incorporations are termed *specific* inasmuch as the selenide atom is always placed in the μ_3-Q site bridging three

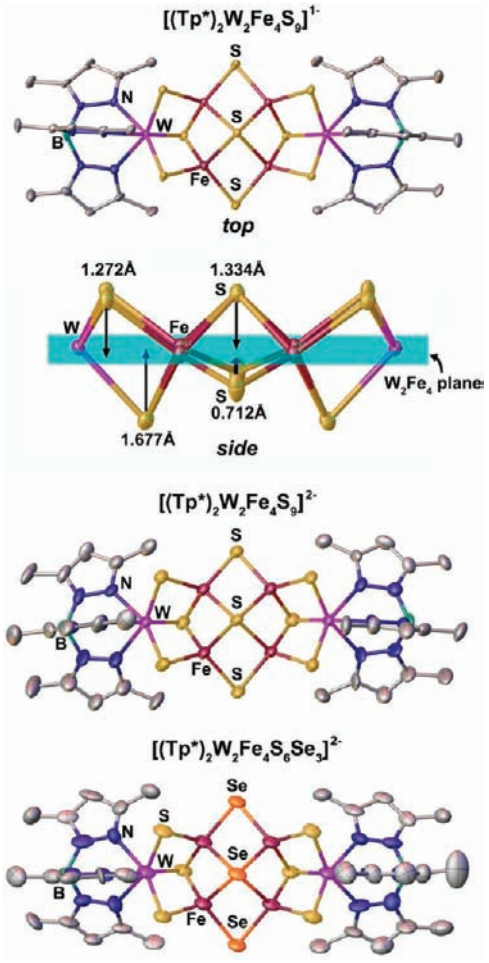

Figure 10. Structures of double-cuboidal clusters **12** (monoclinic form), **13**, and **15** viewed down a real or idealized C_2 axis. The side view of **12** is normal to the W_2Fe_4 plane and shows atom displacements (Å) from that plane.

iron atoms; that is, all of the W−S bonds are preserved in the reduction of tungsten in cluster formation (reaction 5).

2. Edge-Bridged Double Cubanes. The reductive dimerization of single cubanes via reaction 7 produces the EBDCs **8a** and **8b**. The origin of the μ_4-S atoms, which possibly result from sulfide rearrangement within a cubane core upon reduction or scrambling between cores, cannot be addressed from the structure of an all-sulfide cluster. However, the reductive conversion of selenide cluster **7b** to **8b**, which has two μ_4-Se atoms in the $[W_2Fe_6S_6Q_2]^{2+}$ core, supports a pathway involving neither of these events. This result requires that the single-cubane reactants remain intact during reduction, phosphine dissociation, and dimerization, which occurs along Fe−Se edges to recover the observed transoid stereochemistry. It is further probable that the unique sulfur in the precursor cubane assumes the μ_4-S site in the all-sulfide EBDC product.

3. P^N-Type Clusters. The reactions of **8b** with QH^- lead to previously unknown chalcogenide atom rearrangements in the course of cluster formation. Reactions 8 and 9 involve both external and internal reactants. Reactants QH^- induce the rearrangements 2 μ_4-Se → μ_2-Se + μ_6-Se in forming P^N-type cores. Thus, one of the μ_4-Se atoms in the precursor double-cubane assumes the μ_6-Se site and the other a doubly bridging site. The external chalcogenide appears in the products **9** and **10** as a μ_2-Q bridge. The formation of such a bridge is

dx.doi.org/10.1021/ja3010539 | J. Am. Chem. Soc. 2012, 134, 6479−6490

Table 3. Metrical Parameters (Å, deg)[a] of the Double-Cuboidal Clusters $[(Tp^*)_2W_2Fe_4S_6Q_3]^z$ (Q = S, Se)

	$[(Tp^*)_2W_2Fe_4S_6Se_3]$	$[(Tp^*)_2W_2Fe_4S_9]^{1-}$ [b]	$[(Tp^*)_2W_2Fe_4S_6Se_3]^{2-}$ [c]	$[(Tp^*)_2W_2Fe_4S_9]^{2-}$
Fe−(μ_2-S)[d]	2.209(2)	2.217(1)	2.232(2)	2.217(9)
Fe−(μ_2-Q)	2.321(12)	2.194(1)	2.365(3)	2.226(10)
Fe−(μ_3-S)	2.268(14)	2.266(1)	2.296(5)	2.288(10)
Fe−(μ_4-Q)	2.444(8)	2.321(3)	2.463(4)	2.315(9)
Fe···Fe[e]	2.66(3), 2.754(6)	2.646(2), 2.686(2)	2.643(4), 2.881(4)	2.604(2), 2.763(12)
Fe−(μ_2-Q)−Fe	72.9(2), 72.6(1)	75.5(1)	75.4(1), 74.6(1)	76.6(1), 76.8(1)
Fe−(μ_4-Q)−Fe[f]	65.3(2), −68.7(1)	69.51(9), 70.71(9)	64.6(1)−72.2(1)	68.3(1)−73.7(1)
	102.7(1), 103.8(1)	108.3(2), 109.0(2)	104.3(1), 105.9(1)	109.4(2), 110.8(2)
$\delta(\mu_2$-S)[g]	1.21(1), 1.20(1)	1.267(3), 1.276(3)	1.312(6), 1.286(6)	1.269(4), 1.321(5)
	1.27(1), 1.17(1)		1.267(5), 1.351(5)	1.227(5), 1.385(4)
$\delta(\mu_2$-Q)[g]	0.47(1), 0.49(1)	0.712(4)	0.710(4), 0.895(4)	0.702(5), 0.845(5)
$\delta(\mu_3$-S)[g]	1.66(1), 1.70(1)	1.677(3)	1.707(5), 1.718(5)	1.710(4), 1.697(4)
$\delta(\mu_4$-Q)[g]	1.565(6)	1.334(4)	1.462(2)	1.290(4)

[a]Single values are unique or mean values. [b]Monoclinic, C_2 axis; the parameters for the orthorhombic form are very similar except for one (long) Fe···Fe distance of 2.731(1) Å. [c]One of two independent clusters with nearly identical dimensions. [d]Bridge atom bound to W. [e]The longer distance is parallel to the W−(μ_4-Q)−W vector. [f]Larger angles involve opposite atoms. [g]Perpendicular displacement from the W_2Fe_4 mean plane; μ_2-S and μ_4-Q are on one side of the W_2Fe_4 plane and μ_2-Q and μ_3-S on the opposite side.

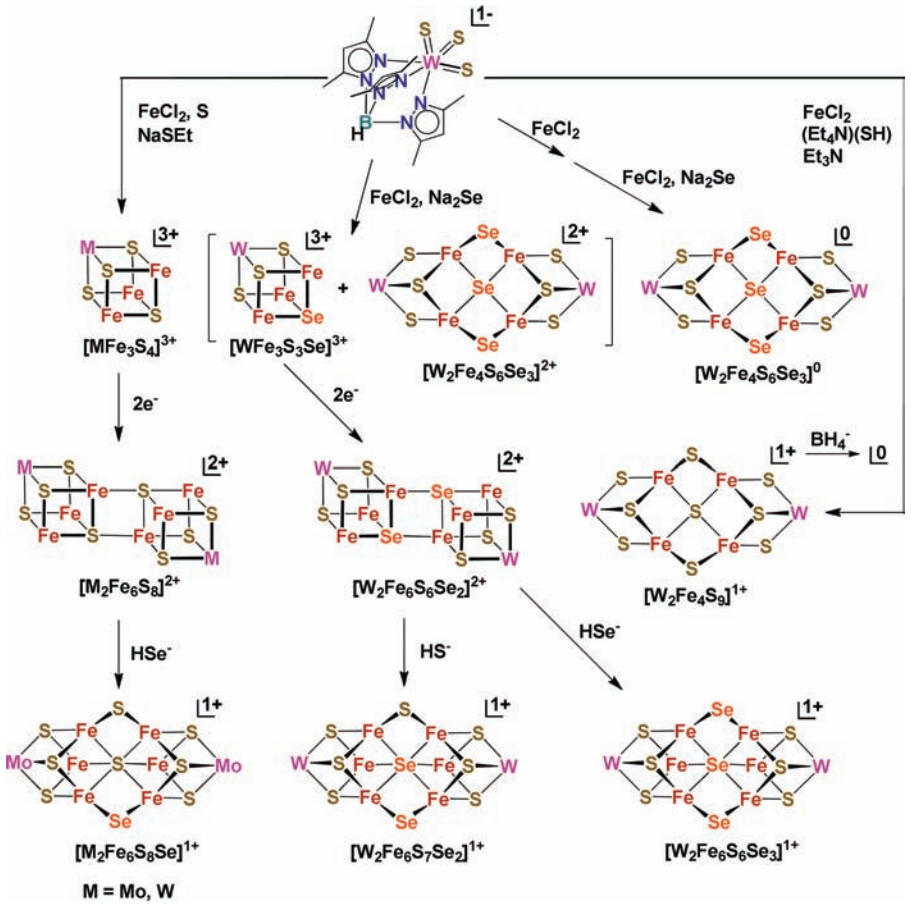

Figure 11. Summary of sulfide and selenide incorporation in the core structures of four cluster types. The core rearrangement in the lower part of the left-hand column is depicted in full in Figure 1.

anticipated by the result of reaction 1 with Q = Se. From these observations, it is probable that a μ_4-S atom in the EBDC precursor assumes the μ_6-S role in the P^N-type cluster product.

4. Double Cuboidal Clusters. The use of Na_2Se in reactions 12 and 13 places selenide in the μ_2-Se and μ_4-Se sites of the $[W_2Fe_4S_6Q_3]^{2+}$ core of double-cuboidal cluster **14**. The WS_3 groups are unaffected. We conclude that in this reaction and the related reaction 11, the three chalcogenide atoms bridging the WFe_2S_3 fragments arise from the sulfide or selenide external reagent.

Summary. The structural roles of external and internal chalcogenide reactants are summarized in Table 4. We consider it highly probable that the positions occupied by selenide in single cubanes, EBDCs, P^N-type clusters, and double-cuboidal

dx.doi.org/10.1021/ja3010539 | J. Am. Chem. Soc. 2012, 134, 6479−6490

Table 4. Chalcogenide Reactant Summary for W−Fe−Q Cluster Synthesis (Q = S, Se)

- Structural fate of *external* chalcogenide reactants:
  - single cubanes: $(\mu_3\text{-Q})Fe_3$
  - P^N-type clusters: $(\mu_2\text{-Q})Fe_2$
  - double-cuboidal clusters: $(\mu_2\text{-Q})Fe_2 + (\mu_4\text{-Q})Fe_4$
- Reactions of *internal* chalcogenide atoms:
  - single cubane → EBDC $(\mu_3\text{-Q})Fe_3 \rightarrow (\mu_4\text{-Q})Fe_4$
  - EBDC → P^N-type $(\mu_4\text{-Q})Fe_4 \rightarrow (\mu_2\text{-Q})Fe_2 + (\mu_6\text{-Q})Fe_6$
- Because all of the W−S bonds are preserved in all of the reactions, the concept of $[(Tp^*)WS_3]^{1-}$ as a *template reactant* is validated.

clusters are same as those assumed by external or internal sulfide in the formation of sulfide-only clusters. The premise is that selenium is a faithful structural surrogate of sulfur in molecules with equal numbers but differing populations of chalcogenides. From this information, it is possible to conceptualize the formation of an EBDC from a single cubane and a P^N-type cluster from an EBDC, as outlined in Figure 11. However, it is not yet possible to propose detailed molecular pathways on the basis of the evidence available. The conversion of a single cubane to an EBDC is perhaps the simplest. Nevertheless, the order of reduction and phosphine dissociation is not known, nor are the details of the dimerization reaction. The conversion of an EBDC to a P^N-type cluster is more complicated because of the larger number of Fe−Q bonds broken and made and the sequence of events in the process. However, any eventual mechanism must conform to the structural fate of the two μ_4-Q atoms of the precursor.

The results with external and internal selenide support the viability of template-assisted cluster assembly. It is noteworthy that in every transformation in Figure 11 (summarized in Table 4), selenide is bound only to iron; that is, the WS_3 template group of precursor **1** remains intact. Furthermore, every cluster contains a WFe_2S_3 fragment, which was separately isolated in the form of incomplete cubanes **3** and **4**. The success of the approach must depend in large part on the greater bond strength and kinetic inertness of the template group. While the bond-strength order $W^{III,IV}$−S > $Fe^{II,III}$−S would appear to be a certainty, there are no appropriate data for comparison. Given the pronounced chemical similarities between tungsten and molybdenum,[53] we anticipate that the results obtained in this work would extrapolate to the corresponding Mo−Fe−S/Se clusters. However, the potential template reactant $[(Tp^*)MoS_3]^{1-}$ needed to test this issue has not been prepared. Lastly, selenide substitution and the associated structural results have served the additional purpose of confirming template-based cluster assembly. The $[(Cp^*)MoS_3]^{1-}$ complex[54] may have similar templating capability, although it has not been directly employed in cluster assembly leading to cubane-type $MoFe_3S_4$ clusters.[55]

■ ASSOCIATED CONTENT

Supporting Information

X-ray crystallographic data in CIF format for all of the compounds in Table S1, the ^{1}H NMR spectrum of **9**, representative Mössbauer spectra, and isomers of EBDCs. This material is available free of charge via the Internet at http://pubs.acs.org.

■ AUTHOR INFORMATION

Corresponding Author

holm@chemistry.harvard.edu

Notes

The authors declare no competing financial interest.

■ ACKNOWLEDGMENTS

This research was supported by NIH Grant GM-28856.

■ REFERENCES

(1) Lee, S. C.; Holm, R. H. *Chem. Rev.* **2004**, *104*, 1135−1157.
(2) Holm, R. H.; Simhon, E. D. In *Molybdenum Enzymes*; Spiro, T. G., Ed.; Wiley: New York, 1985; pp 1−87.
(3) Malinak, S. M.; Coucouvanis, D. *Prog. Inorg. Chem.* **2001**, *49*, 599−662.
(4) Abbreviations are given in Chart 1.
(5) Majumdar, A.; Holm, R. H. *Inorg. Chem.* **2011**, *50*, 11242−11251.
(6) Peters, J. W.; Stowell, M. H. B.; Soltis, S. M.; Finnegan, M. G.; Johnson, M. K.; Rees, D. C. *Biochemistry* **1997**, *36*, 1181−1187.
(7) Mayer, S. M.; Lawson, D. M.; Gormal, C. A.; Roe, S. M.; Smith, B. E. *J. Mol. Biol.* **1999**, *292*, 871−891.
(8) Einsle, O.; Tezcan, F. A.; Andrade, S. L. A.; Schmid, B.; Yoshida, M.; Howard, J. B.; Rees, D. C. *Science* **2002**, *297*, 1696−1700.
(9) Spatzal, T.; Aksoyoglu, M.; Zhang, L.; Andrade, S. L. A.; Schleicher, E.; Weber, S.; Rees, D. C.; Einsle, O. *Science* **2011**, *334*, 940.
(10) Lancaster, K. M.; Roemelt, M.; Ettenhuber, P.; Hu, Y.; Ribbe, M. W.; Neese, F.; Bergman, U.; DeBeer, S. *Science* **2011**, *334*, 974−977.
(11) Jeoung, J.-H.; Dobbek, H. *Science* **2007**, *318*, 1461−1464.
(12) Kung, Y.; Doukov, T. I.; Seravalli, J.; Ragsdale, S. W.; Drennan, C. L. *Biochemistry* **2009**, *48*, 7432−7440.
(13) Amara, P.; Mouesca, J.-M.; Volbeda, A.; Fontecilla-Camps, J. C. *Inorg. Chem.* **2011**, *50*, 1868−1878.
(14) Demadis, K. D.; Campana, C. F.; Coucouvanis, D. *J. Am. Chem. Soc.* **1995**, *117*, 7832−7833.
(15) Zhang, Y.; Holm, R. H. *J. Am. Chem. Soc.* **2003**, *125*, 3910−3920.
(16) Berlinguette, C. P.; Miyaji, T.; Zhang, Y.; Holm, R. H. *Inorg. Chem.* **2006**, *45*, 1997−2007.
(17) Berlinguette, C. P.; Holm, R. H. *J. Am. Chem. Soc.* **2006**, *128*, 11993−12000.
(18) Hlavinka, M. L.; Miyaji, T.; Staples, R. J.; Holm, R. H. *Inorg. Chem.* **2007**, *46*, 9192−9200.
(19) Zuo, J.-L.; Zhou, H.-C.; Holm, R. H. *Inorg. Chem.* **2003**, *42*, 4624−4631.
(20) Scott, T. A.; Holm, R. H. *Inorg. Chem.* **2008**, *47*, 3426−3432.
(21) (a) Seino, H.; Arai, Y.; Iwata, N.; Nagao, S.; Mizobe, Y.; Hidai, M. *Inorg. Chem.* **2001**, *40*, 1677−1682. (b) Seino, H.; Iwata, N.; Kawarai, N.; Hidai, M.; Mizobe, Y. *Inorg. Chem.* **2003**, *42*, 7387−7395.
(22) Hong, D.; Zhang, Y.; Holm, R. H. *Inorg. Chim. Acta* **2005**, *358*, 2303−2311.
(23) In this and other reactions forming P^N-type clusters, 0.5 equiv of dihydrogen is invoked as a default product because the $\{[M_2Fe_6Q_8]^{2+} + S^{2-}\}$ reactants are more reduced than the $[M_2Fe_6Q_9]^{1+}$ product by one electron. The potentials of the $[(Tp)_2Mo_2Fe_6Q_9(QH)_2]^{4-/3-}$ redox couples are −1.8 V vs SCE, making reduced clusters in the $[M_2Fe_6S_9]^0$ oxidation state difficult to isolate in substance.[17]
(24) Zhang, Y.; Holm, R. H. *Inorg. Chem.* **2004**, *43*, 674−682.
(25) Pesavento, R. P.; Berlinguette, C. P.; Holm, R. H. *Inorg. Chem.* **2007**, *46*, 510−516.
(26) Emsley, J. *The Elements*, 3rd ed.; Oxford University Press: Oxford, U.K., 1998.
(27) Yu, S.-B.; Papaefthymiou, G. C.; Holm, R. H. *Inorg. Chem.* **1991**, *30*, 3476−3485.
(28) Reynolds, J. G.; Holm, R. H. *Inorg. Chem.* **1981**, *20*, 1873−1878.
(29) Bobrik, M. A.; Laskowski, E. J.; Johnson, R. W.; Gillum, W. O.; Berg, J. M.; Hodgson, K. O.; Holm, R. H. *Inorg. Chem.* **1978**, *17*, 1402−1410.
(30) Meyer, J.; Moulis, J.-M.; Gaillard, J.; Lutz, M. *Adv. Inorg. Chem.* **1992**, *38*, 73−115.

(31) See the Supporting Information.
(32) Rao, P. V.; Holm, R. H. *Chem. Rev.* **2004**, *104*, 527−559.
(33) Hauser, C.; Bill, E.; Holm, R. H. *Inorg. Chem.* **2002**, *41*, 1615−1624.
(34) Coucouvanis, D.; Stremple, P.; Simhon, E. D.; Swenson, D.; Baenziger, N. C.; Draganjac, M.; Chan, L. T.; Simopoulos, A.; Papethymiou, V.; Kostikas, A.; Petroleas, V. *Inorg. Chem.* **1983**, *22*, 293−308.
(35) Müller, A.; Bögge, H.; Schimanski, U.; Penk, M.; Nieradzik, K.; Dartmann, M.; Krickemeyer, E.; Schimanski, J.; Römer, C.; Römer, M.; Dornfeld, H.; Wienböker, U.; Hellmann, W.; Zimmermann, M. *Monatsh. Chem.* **1989**, *120*, 367−391.
(36) Dumas, E.; Marrot, J.; Jullien, J.; Sécheresse, F. *Inorg. Chim. Acta* **2005**, *358*, 70−76.
(37) Arikawa, Y.; Kawaguchi, H.; Kashiwabara, K.; Tatsumi, K. *Inorg. Chem.* **2002**, *41*, 513−520.
(38) The structure of $(Et_4N)[\mathbf{3}]$ was previously determined with a crystal containing this compound cocrystallized with $(Et_4N)[\mathbf{5a}]$.[22] The structure reported here was obtained with a pure crystal and is of improved quality.
(39) Fomitchev, D. V.; McLauchlan, C. C.; Holm, R. H. *Inorg. Chem.* **2002**, *41*, 958−966.
(40) Osterloh, F.; Segal, B. M.; Achim, C.; Holm, R. H. *Inorg. Chem.* **2000**, *39*, 980−989.
(41) Xi, B.; Holm, R. H. *Inorg. Chem.* **2011**, *50*, 6280−6288.
(42) Chen, X.-D.; Duncan, J. S.; Verma, A. K.; Lee, S. C. *J. Am. Chem. Soc.* **2010**, *132*, 15884−15886.
(43) The term "cuboidal" was originally applied in this laboratory to the incomplete cubane structure $Fe_3S_4 = Fe_3(\mu_2\text{-}S)_3(\mu_3\text{-}S)$.[51] Here it is applied to $WFe_2(\mu_2\text{-}Q)_2(\mu_3\text{-}S)(\mu_4\text{-}Q)$, two of which have a common vertex $(\mu_4\text{-}Q)$.
(44) Christou, G.; Holm, R. H.; Sabat, M.; Ibers, J. A. *J. Am. Chem. Soc.* **1981**, *103*, 6269−6271.
(45) Christou, G.; Sabat, M.; Ibers, J. A.; Holm, R. H. *Inorg. Chem.* **1982**, *21*, 3518−3526.
(46) Henkel, G.; Strasdeit, H.; Krebs, B. *Angew. Chem., Int. Ed. Engl.* **1982**, *21*, 201−202.
(47) Strasdeit, H.; Krebs, B.; Henkel, G. *Inorg. Chem.* **1984**, *23*, 1816−1825.
(48) Fan, Y.; Guo, C.; Zhang, Z.; Liu, X. *Sci. Sin., Ser. B* **1988**, *31*, 161−170.
(49) Holm, R. H.; Hagen, K. S.; Watson, A. D. In *Chemistry for the Future*; Grünewald, H., Ed.; Pergamon: New York, 1984; pp 115−124.
(50) Strasdeit, H.; Krebs, B.; Henkel, G. *Z. Naturforsch.* **1987**, *42b*, 565−572.
(51) Zhou, J.; Hu, Z.; Münck, E.; Holm, R. H. *J. Am. Chem. Soc.* **1996**, *118*, 1966−1980.
(52) Zhou, H.-C.; Su, W.; Achim, C.; Rao, P. V.; Holm, R. H. *Inorg. Chem.* **2002**, *41*, 3191−3201.
(53) Holm, R. H.; Solomon, E. I.; Majumdar, A.; Tenderholt, A. *Coord. Chem. Rev.* **2011**, *255*, 993−1015.
(54) Kawaguchi, H.; Yamada, K.; Lang, J.-P.; Tatsumi, K. *J. Am. Chem. Soc.* **1997**, *119*, 10346−10358.
(55) Komuro, T.; Kawaguchi, H.; Lang, J.; Nagasawa, T.; Tatsumi, K. *J. Organomet. Chem.* **2007**, *692*, 1−9.